# Structural and electromagnetic properties of yttrium-substituted Ni-Zn ferrites

Silvia E. Jacobo[1] and Paula G. Bercoff[2]*

[1]DiQuiMMAI. Facultad de Ingeniería, UBA. INTECIN-Conicet. Av. Paseo Colón 850. Buenos Aires. Argentina.

[2]FaMAF, Universidad Nacional de Córdoba. IFEG-Conicet. Ciudad Universitaria. Córdoba. Argentina.

*Corresponding author: Dr. Paula G. Bercoff
  FaMAF, UNC. IFEG, Conicet.
  M. Allende s/n. Ciudad Universitaria.
   5000 Córdoba, Argentina
  Tel: +54 351 433 4051 (ext. 103)
   Fax: +54 351 433 4054
  e-mail: bercoff@famaf.unc.edu.ar

## Abstract

The effect of $Y^{3+}$ substitution on the structural and magnetic properties of $Ni_{0.5}Zn_{0.5}Y_yFe_{2-y}O_4$ ($0.01 \leq y \leq 0.05$) was investigated. Microwave absorption properties of these ferrites in the frequency range 1 MHz to 1.8 GHz were also studied. Yttrium substitution slightly reduces crystallite sizes and cell parameters, and modifies saturation magnetization, permeability and permittivity in the explored frequency range. The dielectric constant decreases with yttrium content, showing a constant behavior in the explored frequency range. The maximum of the magnetic losses diminishes and shifts to higher frequencies with yttrium inclusion. Yttrium-substituted Ni-Zn ferrites (with Y content ≤0.05 per formula unit) can be considered good attenuator materials in the explored microwave range.

Keywords: Ni-Zn ferrites; Yttrium-doped ferrites; Microwave Attenuation.

## 1. Introduction

Ni–Zn ferrites are suitable materials for high frequency applications up to a few hundreds of MHz because of their high electrical resistivity, low eddy current and reduced dielectric losses [1]. These ferrites are used in radio frequency circuits, high-quality filters, rod antennas, microwave devices, magnetic fluids, transformer cores, read/write heads for high-speed digital tapes and operating devices [2–4].

Higher values of electrical resistivity could be achieved by doping these ferrites with proper divalent cations, as well as by controlling their microstructures. It is mentioned that ultra-fine grains would provide a large number of grain boundaries which may act as a barrier for electron flow, resulting in the reduction of eddy current losses [5].

The effect of substitutions with different elements such as Ti [6], Ge [7], Cu [8]or rare earths [9] on the electrical and magnetic properties of Ni–Zn ferrites has also been reported. It is found that the occupation of rare earth ions in octahedral (B) sites prevents the motion of $Fe^{2+}$ in the conduction process, thus causing an increase in resistivity [9].

Some considerations must be taken into account due to the large size of the earth ions. Atheia et al. [10], reported that there is a solubility limit of rare ions in the spinel lattice and that introducing a relatively small amount of $La_2O_3$ instead of $Fe_2O_3$ causes a significant change in the electrical and magnetic properties. From these studies, it has been inferred that the choices of the substitution and composition favorably influence the magnetic and electrical properties of ferrites. As a result, it is possible to obtain a good soft magnetic material by optimally choosing the substitutions.

We have earlier explored some structural and magnetic properties for low-doping rare earths (RE) in Ni-Zn ferrites prepared by the sol-gel method. We reported that the inclusion of much larger ionic radii RE ions results in local distortion and disorder that induces an important softening of the lattice [11, 12].

In this work, we report the structural and magnetic properties of $Ni_{0.5}Zn_{0.5}Y_yFe_{2-y}O_4$ for $y$=0.0; 0.01, 0.02 and 0.05, as well as the influence of $Y^{3+}$ substitution on the microwave absorption properties in the frequency range 1 MHz to 1.8 GHz. Samples were prepared by sol-gel followed by a citrate-nitrate self-combustion process in order to obtain the substituted ferrites at a relatively low temperature. Yttrium was selected as a doping element because of its diamagnetic condition as $Y^{3+}$ and other interesting properties reported earlier [11]. Although there are some works

related to the structural characteristics of these materials, to the best of our knowledge, this work presents novel results related to microwave properties in the range 1MHz-1.8 GHz.

## 2. Experimental

Samples were prepared by the sol-gel method as it was earlier reported in Ref. [12]. The corresponding proportions to prepare $Ni_{0.5}Zn_{0.5}Fe_2O_4$ from iron nitrates, nickel and zinc oxalates were weighed according to the required stoichiometric proportions and diluted in water. A 3M citric acid solution (50 ml) was added to each metal solution (50 ml) and heated at 40°C for approximately 30 min, under continuous stirring. The final mixture was slowly evaporated until a highly viscous gel was formed. For the preparation of the yttrium-doped samples, Y(III) nitrates were used, being previously dissolved in 3M citric acid solutions. The final residue was calcined at 1100°C for 3 h. The resulting samples, $Ni_{0.5}Zn_{0.5}Y_yFe_{2-y}O_4$ with nominal values $y$=0.0; 0.01; 0.02 and 0.05 were labeled Y0, Y1, Y2 and Y5, respectively.

X-ray diffraction (XRD) powder diffractograms were measured with a Philips PW 3860 diffractometer, in the 2θ range 20 to 70 °, with a step size of 0.02 °, for 6 s per step. A Sigma Zeiss Field Emission scanning electron microscope (LAMARX facilities) was used to characterize the morphology of the samples. The magnetic properties were measured with a Lakeshore 7300 vibrating sample magnetometer, at room temperature, with a maximum applied field of 1.5 T.

The powders were pressed without binder into toroidal rings and pellets at a pressure of 2 tons and sintered in air at 1100°C for 2 h, followed by a slow cooling in the furnace. Complex permeability of toroids and complex permittivity of pellets were measured on a HP4291A Material Analyzer from 1 to 1800MHz.

## 3. Results and discussion

### 3.1 Structural characterization

Figure 1 shows the X-ray diffractograms of the series $Ni_{0.5}Zn_{0.5}Y_yFe_{2-y}O_4$ ($y$=0.0, 0.01, 0.02 and 0.05). The observed peaks correspond only to the spinel phase and no secondary phases are apparent, within the detection limit of this technique.
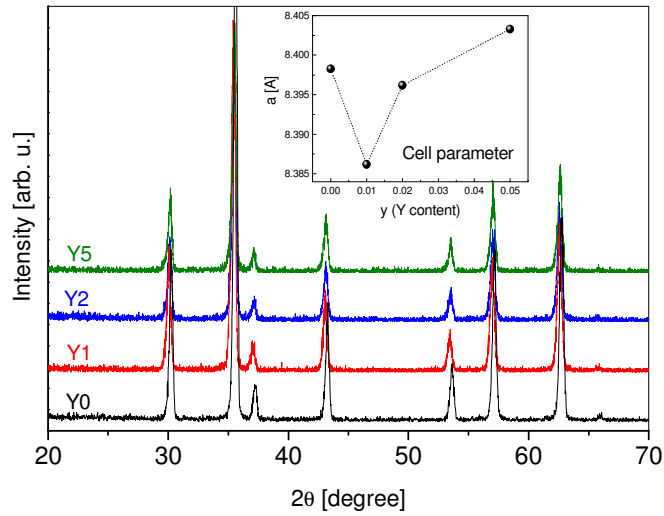
Figure 1. X ray diffractograms of samples Y0, Y1, Y2 and Y5. In every case the peaks correspond to the spinel phase, showing no secondary phases. The inset displays the change in cell parameter with yttrium content.

Cell parameters $a$ and crystallite sizes $D$ for each sample were obtained from the spectra refinement and the Williamson–Hall extrapolation, with the aid of the software Powder Cell. Crystallite sizes are slightly reduced with yttrium substitution from 28 nm for Y0 to 26 nm for Y1. This value remains almost constant for the samples with higher substitutions (see Table 1).

Table 1: Samples denomination, nominal composition, crystallite size $D$ and cell parameter $a$.

| Sample | Nominal composition | $D$ [±2 nm] | $a$ [A] |
|---|---|---|---|
| Y0 | $Ni_{0.5}Zn_{0.5}Fe_2O_4$ | 28 | 8.3983(2) |
| Y1 | $Ni_{0.5}Zn_{0.5}Y_{0.01}Fe_{1.99}O_4$ | 26 | 8.3862(2) |
| Y2 | $Ni_{0.5}Zn_{0.5}Y_{0.02}Fe_{1.98}O_4$ | 25 | 8.3962(3) |
| Y5 | $Ni_{0.5}Zn_{0.5}Y_{0.05}Fe_{1.95}O_4$ | 26 | 8.4033(5) |

The cell parameter first slightly decreases with yttrium inclusion in the lattice and then increases for higher substitutions, as shown in the inset of Figure 1 and Table 1. It is well known that the lattice parameter $a$ is strongly dependent on the $RE^{3+}$ ionic radii and the cationic distribution among the interstitial A and B sites of the spinel lattice. In a typical inverse spinel structure, the introduction of a given amount of $RE^{3+}$ cations into the octahedral sites should increase the value of $a$ compared to the unsubstituted $NiZnFe_2O_4$ ferrite. The observed decrease in $a$ with increasing substitution can be explained considering the ions redistribution between the

available interstitial tetrahedral (A) and octahedral (B) sites of the spinel lattice. Another plausible explanation for the observed decrease in lattice parameters may be originated from possible iron vacancies in the samples during the crystallization process, due to the introduction of a large ion size in the octahedral site [13].

Another observed effect of yttrium substitution is the reduction in the samples' particle size. The mean particle size of sample Y0 is 350 nm, while for the substituted samples it is 90 nm, and is rather independent of $y$. Figure 2 shows SEM images of Y0 and Y1 (the morphology of both Y2 and Y5 is very similar to Y1, and images are not shown). According to the obtained crystallite sizes from XRD results and the observed particle sizes, it is deduced that the particles of sample Y0 are polycrystalline and the substituted samples are composed of single-crystal particles. The effect of particle size reduction when doping with rare earths has been observed by other authors in different systems (see, for instance, Refs. 14 and 15) and it is attributed to the substitution by the $RE^{3+}$ ions that lead to lattice strains and a disordered lattice structure. These changes restrain grain crystallization and hinder the grain growth, therefore decreasing the crystallite sizes.
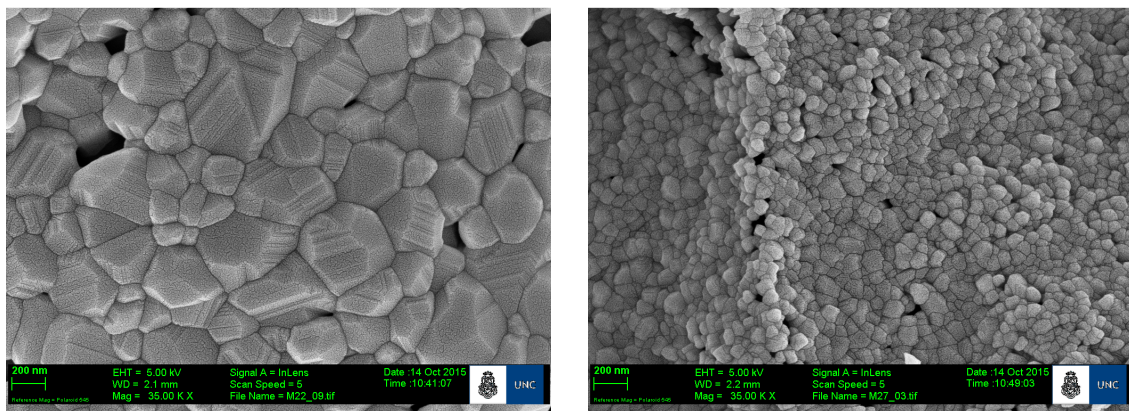


Figure 2. SEM images of sample Y0 (left) and Y1 (right). Being taken with the same magnification, the particle size reduction in the doped sample is evident.

### 3.2 Magnetic characterization

The first quadrant of the measured hysteresis loops is shown in Figure 3, where the decrease of saturation magnetization ($M$s) with yttrium content can be noticed. Saturation is attained at relatively low fields in every case. Coercivity $H$c is very low for all samples and increases with $y$,

consistently with the particle size decrease (see inset of Figure 3). This decrease in magnetization with yttrium inclusion is similar to the reported by V. Jancárik et al. [16], who also observe an increase in coercivity with Y substitution. They related these results with a reordering of ions in both sublattices of the spinel structure, due to the large difference between ionic radii of Y and Fe.
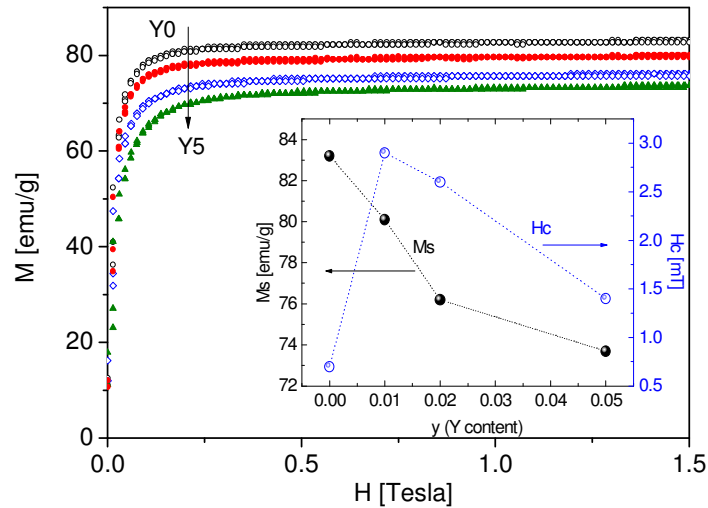


Figure 3. First quadrant of the hysteresis loops, corresponding to samples Y0 to Y5. The inset shows saturation magnetization (Ms) and coercivity (Hc) values for samples with different Y content.

The decrease in $M$s can only be explained considering that $Y^{3+}$ ions (with no net magnetic moment) enter the spinel lattice in octahedral sites and produce a redistribution of the cations in the available interstitials that dilutes the exchange interactions and therefore, the total magnetic moment of the ferrite.

**3.3 Electromagnetic properties**

Complex permittivity ( $\varepsilon = \varepsilon' - j\varepsilon''$) and complex permeability ($\mu = \mu' - j\mu''$) represent the dielectric and dynamic magnetic properties of magnetic materials. The real parts of $\varepsilon$ and $\mu$ symbolize the storage capability of electric and magnetic energy. The imaginary parts represent the loss of electric and magnetic energy through tan $\delta_M = \mu''/\mu'$ and tan $\delta_D = \varepsilon''/\varepsilon'$.

Figure 4 displays the permittivity of the yttrium ferrite samples in the microwave range 1 MHz-1.8 GHz.
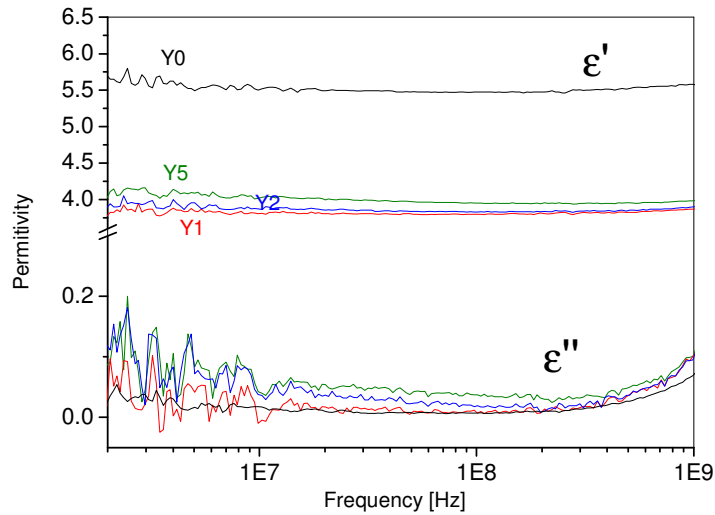
**Figure 4.** Dependence of permittivity ε (real (ε') and imaginary (ε'') contributions) as a function of frequency.

It is clear from Figure 4 that the un-doped sample (Ni–Zn ferrite) has the maximum value of permittivity (ε), which means it has both a maximum polarization as well as a maximum valence exchange. The dielectric constant decreases with yttrium substitution, showing a constant behavior in the explored frequency range. The mechanism of polarization in polycrystalline ferrites is reported to be mainly hopping of electrons between ions of the same element, but in different oxidation states, such as $Fe^{2+} \rightarrow Fe^{3+} + e^-$ [17, 18].

As the electrons reach the grain boundaries on application of an electric field, they pile up and a charge build-up takes place, causing interfacial polarization. Because the ferrites are sintered at a relative low temperature during a short time, the possibility that ions exist in different valance states is rather low, reducing thereby the probability of electron hopping and hence of polarization, resulting in a low dielectric constant. Electrical conductivity was found to decrease with yttrium content in $Ni_{0.5}Zn_{0.5}Y_yFe_{2-y}O_4$, which is related to the decrease in permittivity [19]. This can be attributed to the change in resistivity of the samples, since in ferrites the dielectric constant is inversely proportional to the square root of resistivity [20]. Yttrium ions do not participate in the conduction process but limit the degree of $Fe^{2+}$–$Fe^{3+}$ conduction by blocking up the $Fe^{2+}$–$Fe^{3+}$

transformation, thus resulting in a decrease in conductivity. Similar results were reported by E. E. Ateia et al. for Mn-Zn ferrite with other RE ions [21]. The probable reason for this behavior is that the substitution induces more electric dipoles, so the imaginary part of the relative complex permittivity increases [22].

It is usually believed that the dielectric loss mainly consists of the electron polarization, the ion polarization, and the electric dipolar polarization. For electron and ion polarizations, the losses are relatively weak in the microwave range and strongly occur at higher frequencies [23]. Thus, we can deduce that the dielectric loss of all the studied samples results mainly from the electric dipolar polarization. In the polarization process, plenty of electro-magnetic (EM) energy is irreversibly transformed to Joule thermal energy.

As magnetic losses are related to the absorption effect, $\tan \delta_M$ profiles versus frequency were analyzed (Figure 5). For all compositions, $\tan \delta_M$ steeply increases for frequencies higher than 1 GHz.
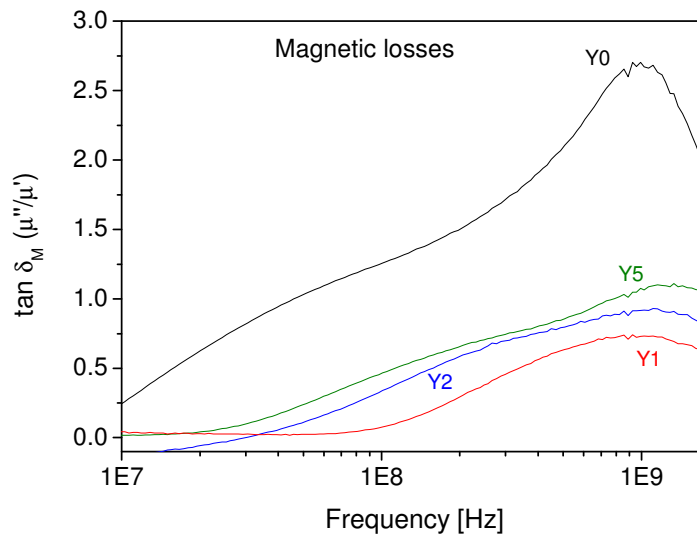


**Figure 5.** Dependence of magnetic losses ($\tan\delta_M = \mu''/\mu'$) with frequency.

According to the ferromagnetic theory [24], the natural resonance frequency is determined by the magnetocrystalline anisotropy field ($H_A$) and the imaginary part of permeability ($\mu''$) is related to saturation magnetization.

The expression for μ'' is proportional to $M$s and inversely proportional to $H_A$:

$$\mu'' = \frac{M_S}{2\mu_0 H_A \alpha} \qquad (1)$$

where $\alpha$ is the Gilbert damping coefficient. Being $H_A = 2K_1/M_S$, equation (1) can be rewritten as:

$$\mu'' = \frac{M_S^2}{4\mu_0 K_1 \alpha} \approx \frac{M_S^2}{H_C} \qquad (2)$$

where $\mu_0$ is the permeability of vacuum, and $K_1$ is the anisotropy constant. So, according to equation (2), the values of μ'' decrease with a decrease in $M$s and/or an increase in $H$c. Both phenomena are present in these samples (see the experimental values of $M$s and $H$c for the studied samples in the inset of Figure 3).

The maximum of the magnetic losses diminishes and shifts to higher frequencies with yttrium inclusion.

In the case of a metal-backed single-layered absorber, the reflection loss ($R_L$) for the zero reflection condition can be described with the following relation [25]:

$$R_L (dB) = 20\log\left|Z_{in} - 1\right|/\left|Z_{in} + 1\right|, \qquad (3)$$

being $Z_{in}$ the relative impedance of the sample calculated as:

$$Z_{in} = \sqrt{\mu/\varepsilon}\, \tanh\left[-j(2\pi f D/c)\left(\sqrt{\mu\varepsilon}\right)\right] \qquad (4)$$

where c is the velocity of light ($3 \times 10^8$ m/s), $D$ is the sample thickness ($1.00 \pm 0.05$ mm) and $f$ is the frequency (Hz).

Figure 6 shows the dependence of reflection loss $R_L$ on frequency, with y as a parameter. For lower yttrium content, the maximum $R_L$ is shifted to higher frequencies ($3 \times 10^8$ Hz) while for higher y values, a slight shift towards lower frequencies is observed. A value of $|R_L|$ greater than 20 dB means that the material absorbs 99% of the input power. It can been observed that $|R_L|$ values for all the samples are above 40 dB. These results can be related to promising shielding properties. The samples show excellent absorption properties in a relatively wide bandwidth in the frequency region from 2 MHz to 30 MHz. The high sensibility to the amount of yttrium inclusion makes this system adequate for tuning the absorption properties quite at will.
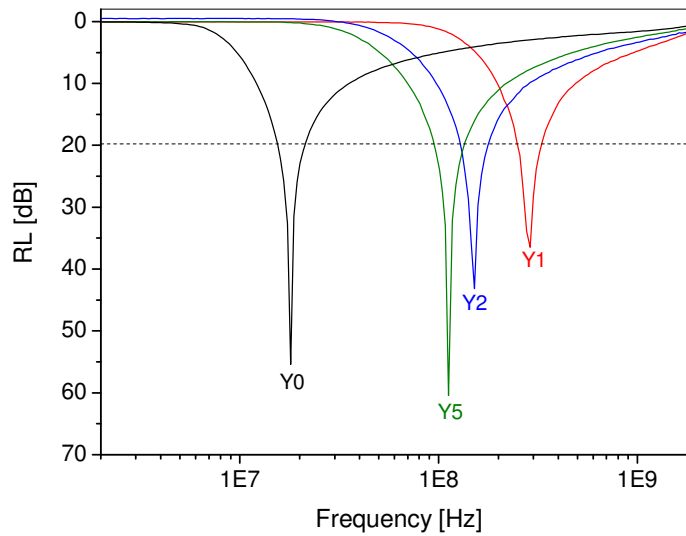
**Figure 6.** Frequency dependence of reflection loss ($R_L$) of $Ni_{0.5}Zn_{0.5}Y_x Fe_{2-x}O_4$. The dashed line indicates the 20 dB limit from which the material absorbs 99% of the input power.

## 4. Conclusions

Y-substituted Ni-Zn ferrites were successfully prepared by the self-combustion method and the influence of $Y^{3+}$ was analyzed. XRD confirms the spinel phase for all compositions, with no segregation of secondary phases. It is remarkable that this preparation method increases yttrium solubility even with relative short thermal treatments. Saturation magnetization slightly decreases with Y substitution. Yttrium doping plays an important role in changing the structural and magnetic properties of these Ni-Zn ferrites, also modifying the attenuation properties. As the $|R_L|$ values for all the samples are above 40dB, they can all be considered as good attenuator materials. These characteristics suggest that high-frequency devices, such as single-layered electromagnetic wave shielding with tailored properties, can be designed using these polycrystalline Y-substituted Ni-Zn ferrites.

## Acknowledgements

## References

[1] L. Li, X. Tu, L. Peng, X. Zhu, "Structure and static magnetic properties of Zr-substituted NiZn ferrite thin films synthesized by sol–gel process", J. All. Comp. 545 (2012) 67–69.

[2] J. J. Thomas, A. B. Shinde, P. S. R. Krishna, N. Kalarikkal, "Cation distribution and micro level magnetic alignments in the nanosized nickel zinc ferrite" J. All. Comp. 546 (2013) 77–83.

[3] Qian Chen, Piyi Du, Wenyan Huang, Lu Jin, Wenjian Weng and Gaorong Han, "Ferrite with extraordinary electric and dielectric properties prepared from self-combustion technique ", Appl. Phys. Lett. 90 (2007) 132907.

[4] Kh. Gheisari, Sh. Shahriari, S. Javadpour, " Structure and magnetic properties of ball-mill prepared nanocrystalline Ni–Zn ferrite powders at elevated temperatures", J. All. Comp. 552 (2013) 146–151.

[5] A. Verma, T.C. Goel, R.G. Mendiratta, M.I. Alam, "Dielectric properties of NiZn ferrites prepared by the citrate precursor method", Mater. Sci. Eng. 60 (1999) 156–162.

[6] E. Rezlescu, N. Rezlescu, C. Pasnicu, M.L. Craus, " Nickel-zinc ferrites with Ti-Ge substitutions for high-frequency use", Ceram. Int. 19 (1993) 71-75.

[7] N. Rezlescu, E. Rezlescu, C. Pasnicu, M.L. Craus, Effects of the rare-earth ions on some properties of a nickel-zinc ferrite", J. Phys.:Condens. Matter 6 (1994) 5707.

[8] M. S. Ruiz, P. G. Bercoff, S. E. Jacobo, "Shielding properties of CuNiZn ferrite in the radio frequency range", Ceram. Int. 39 (2013) 4777-4782.

[9] M. F. Huq, D. K. Saha, R. Ahmed, Z. H. Mahmood, J. Sci. Res. Ni-Cu-Zn Ferrite Research: A Brief Review "", vol. 5 No. 2 (2013) 215-234.

[10] E. E. Ateia, M. A. Ahmed, L. M. Salah, A. A. El-Gamal, "Effect of rare earth oxides and $La^{3+}$ ion concentration on some properties of Ni–Zn ferrites", Physica B 445 (2014) 60–67.

[11] S. E. Jacobo, S. Duhalde, H. R. Bertorello, "Rare earth influence on the structural and magnetic properties of NiZn ferrites", J. Magn. Magn. Mater. 272 (2004) 2253-2254.

[12] E. E. Sileo, R. Rotelo, S. E. Jacobo, "Nickel zinc ferrites prepared by the citrate precursor method", Physica B 320 (2002) 257–260.

[13] Y.Y. Meng, Z.W. Liu, H.C. Dai, H.Y. Yu, D.C. Zeng, S. Shukla, R.V. Ramanujan, "Structure and magnetic properties of $Mn(Zn)Fe_{2-x}RE_xO_4$ ferrite nano-powders synthesized by co-precipitation and refluxing method ", Powder Technol. 229 (2012) 270–275.

[14] X. Zhao, W. Wang, Y. Zhang, S. Wu, F. Li, J. Ping Liu, "Synthesis and characterization of gadolinium doped cobalt ferrite nanoparticles with enhanced adsorption capability for Congo Red", Chem. Eng. Journal 250 (2014) 164–174.

[15] Zhijian Peng , Xiuli Fu, Huilin Ge, Zhiqiang Fu, Chengbi Wang, Longhao Qi, Hezhuo Miao, "Effect of $Pr^{3+}$ doping on magnetic and dielectric properties of Ni–Zn ferrites by "one-step synthesis" ", J. Magn. Magn. Mat. 323 (2011) 2513–2518.

[16] V. Jancárik, E. Usák, M. Soka, M. Usáková, "Magnetic Properties of Yttrium-Substituted NiZn Ferrites", Proceedings of the 15th Czech and Slovak Conference on Magnetism, Kosice, Slovakia, June 17-21 2013, ACTA PHYSICA POLONICA A.

[17] M. A. Amer, O. M. Hemeda, S. A. Olofa, M. A. Henaish, "Thermal properties of the ferrite system $Co_{0.6}Zn_{0.4}Cu_xFe_{2-x}O_4$", Appl. Phys. Comm. 13, 3–4 (1994) 255-263.

[18] P. V. Reddy, T. Seshagiri Rao, "Dielectric behaviour of mixed Li-Ni ferrites at low frequencies", J. Less-Common Met. 86, (1982) 255-261.

[19] S. E. Jacobo, W. G. Fano, A. C. Razzitte, "The effect of rare earth substitution on the magnetic properties of $Ni_{0.5}Zn_{0.5}M_xFe_{2-x}O_4$ (M: rare earth)", Physica B 320 (2002) 261–263.

[20] A. M. Shaikh, S. S. Bellard, B. K. Chougule, "Temperature and frequency-dependent dielectric properties of Zn substituted Li–Mg ferrites", J. Mag. Magn. Mater. 195 (1999) 384–390.

[21] E. Ateia, M. A. Ahmed, A. K. El-Aziz, "Effect of rare earth radius and concentration on the structural and transport properties of doped Mn–Zn ferrite", J. Magn. Magn. Mat. 311 (2007) 545–554.

[22] N. Chen, M. Gu, "Microstructure and Microwave Absorption Properties of Y-Substituted Ni-Zn Ferrites", Open Journal of Metal, 2 (2012) 37-41. doi:10.4236/ojmetal.2012.22006.

[23] A. Thakur, P. Mathur, M. Singh, "Study of dielectric behaviour of Mn–Zn nano ferrites", J. Phys. Chem. Solids 68 (2007) 378–381.

[24] Wang Jing, Zhang Hong, Bai Shuxin, Chen Ke, Zhang Changrui, "Microwave absorbing properties of rare-earth elements substituted W-type barium ferrite", J. Magn. Magn. Mat., 312 (2007) 310-313.

[25] J. Shin, J. H. Oh, "The microwave absorbing phenomena of ferrite microwave absorbers", IEEE Trans. Mag. 29, 6 (1993) 3437-3439.